J Ther Eng, Vol. 10, No. 3, pp. 599−612, May, 2024

Journal of Thermal Engineering
Web page info: https://jten.yildiz.edu.tr
DOI: 10.14744/thermal.0000823

Research Article

Energy, exergy and economic analysis of ammonia-water power cycle coupled with trans-critical carbon di-oxide cycle

Ayoushi SRIVASTAVA[1], Mayank MAHESHWARI[2,*]

[1]*Department of Mechanical Engineering, BBD University, Lucknow, 226028, India*
[2]*Department of Mechanical Engineering, Allenhouse Institute of Technology, Kanpur, 208008, India*

ARTICLE INFO

Article history
Received: 07 March 2023
Accepted: 08 August 2023

Keywords:
Ammonia Water Mixture; First Law Efficiency; Heat Recovery Vapor Generator; Irreversibility; Second Law Efficiency; Trans Critical Carbon Dioxide

ABSTRACT

Power plant engineers today are primarily focused on maximizing the extraction of fuel energy. This objective involves improving the efficiencies of different thermodynamic elements and the overall cycle in terms of both first and second laws of thermodynamics. To achieve this, engineers are employing various techniques aimed at increasing these efficiencies. In the present work, one such technique being utilized is the substitution of water/steam with a different working fluid. By changing the working fluid, engineers aim to optimize the thermodynamic performance of the power plant. In this study, the analysis focuses on the utilization of an ammonia-water mixture combined with Trans critical carbon dioxide in a heat recovery vapor generator. The results of this research reveal that the highest work output and second law efficiency achieved are 1192 kJ/sec and 81.68% respectively. These optimal values are obtained when the topping cycle pressure is set to 50 bar, and the turbine inlet temperatures are 500°C and 300°C for the ammonia-water mixture and Trans critical carbon dioxide respectively. Furthermore, the maximum first law efficiency of 43.57% is observed when the topping cycle pressure is set to 50 bar, the bottoming cycle pressure is set to 160 bar, and the turbine inlet temperature is 300°C. The analysis also reveals that the heat source is responsible for the majority of energy destruction, with a maximum of 1970 kJ/sec of available energy being destroyed at a temperature of 500°C. To achieve the highest values of thermodynamic performance parameters, it is recommended to maintain low pressure in the absorber and condenser. Additionally, the analysis indicates that the cost of electricity generation reaches its peak when the condenser pressure is set at 70 bar, amounting to 0.050 USD/kWh.

Cite this article as: Srivastava A, Maheshwari M. Energy, exergy and economic analysis of ammonia-water power cycle coupled with trans-critical carbon di-oxide cycle. J Ther Eng 2024;10(3):599−612.

INTRODUCTION

Since its inception, available energy is given prime focus by a power plant engineer. Various methods are used to enhance both the efficiencies, change of working fluid is one of the methods used to increase these efficiencies. Among the various fluids used, ammonia-water mixture [1] and super critical carbon dioxide [2,3] had shown an

***Corresponding author.**
*E-mail address: mayankmaheshwari80@rediffmail.com

This paper was recommended for publication in revised form by Editor-in-Chief Ahmet Selim Dalkılıç

Published by Yıldız Technical University Press, İstanbul, Turkey

increase in efficiencies as compared to steam cycle [4,5]. The present literature review is divided into two parts:

- First part reviews the literature on super critical/ trans-critical carbon dioxide cycle
- Literature review on ammonia-water cycle is presented in second part.

Literature Review on Supercritical/Trans-Critical Carbon Dioxide Cycle

Dostal et al. [6] suggested the use of Brayton cycle using sCO_2 as working fluid because of higher efficiencies obtained at lower temperature as compared to helium Brayton cycle. Although the authors raise the corrosion issue due to CO_2 on gas turbine structure. Achieving of higher efficiency at low temperature by sCO_2 was also reported by various authors [7,8].

Dostal et al. [9] further suggested the use of recompression sCO_2 for any type of nuclear reactor when compared to steam cycle or helium Brayton cycle. In a solar driven sCO_2 based on Rankine cycle condensing temperature has more effect on cycle efficiency rather than solar collector efficiency Moreover, using solar collectors for power generation using sCO_2, the temperature lower than 250°C should be used [10,11].

Chen et al. [12] compared ORC (R123) with CO_2 transcritical power cycle. The authors concluded that due to better temperature match between CO_2 and flue gases, transcritical CO_2 cycle shows higher potential as compared to ORC. Similar results were obtained by Michael et al. [13]. Jeong et al. [14] also proposed that cycle efficiency of power cycle using sCO_2 as working fluid can be improved if critical temperature of the fluid is lowered, this can be achieved by identifying CO_2 mixtures having low critical temperatures.

Wang et al. [15] optimized the sCO_2 cycle using genetic algorithm and artificial neural network, the authors concluded that parameters that effect the second law efficiency are turbine inlet pressure, turbine inlet temperature and environment temperature. Li et al. [16] concluded that condensers and recuperates should also be optimized from exergy point of view. The authors further proposed that mixture of CO_2 should be explored in order to increase the system efficiency. Crespi et al. [17] reviewed various papers on sCO_2 ranging from stand-alone cycle to combined cycles, the authors concluded that although sCO_2 shows a potential to replace steam/water cycle but there should be standard set of operating conditions on which the performance of all the cycles can be measured.

Liao et al. [18] concluded that design of turbo machinery for sCO_2 is still in its preliminary stage and exhaustive experimental work should be done on these turbo machines so that the efficiency of the cycle can be increased. Mohammadi et al. [19] analyzed a triple power cycle in which the exhaust from the gas turbine was utilized in driving an ORC and a sCO_2. The authors concluded that pressure increase in the Brayton cycle shows only marginal increase in overall efficiency as compared to increase in turbine inlet temperature.

Thermodynamic and thermo economic comparison of T-CO2, sCO_2 and ORC with a simple Rankine cycle was made by Habibollahzade [20]. The authors concluded that the T-CO_2 can generate the highest power and it has the lowest payback period among all the cycles considered. Yilmaz et al.[21] investigated an integrated plant, comprising of steam turbines, a trans critical carbon dioxide Rankine cycle, a electrolyze, a domestic water heater , and a dryer. Authors concluded an energetic and exergetic efficieny of tCO2-RC sub-plant's performance is as 6.18% and 27.14%, respectively

Other than power generation CO_2 is also used as refrigeration purpose, Sánchez et al. [22] analyze five binary mixtures of CO_2 with the refrigerants R32, R152a, R1234yf, R1234ze (E) and R1270 to obtain the optimum mixture ratio for maximizing COP of tCO_2

Literature Review on Ammonia-Water Cycle

Ammonia-water system of fluid is used as refrigerant for more than a century. Kalina [1] proposed it to be used as an alternate to water/steam. Xu and Goswami [23] proposed relations based on Gibbs free energy to evaluate the properties of the ammonia water mixture.

Cao et al. [24] analyzed a combined power and cooling cycle by using ammonia and water mixture. The authors concluded that with an increase in expander inlet temperature the second law efficiency increases and HRSG forms the highest source of exergy destruction. Various authors [25-27] concluded the superiority of ammonia water mixture over Rankine cycle, in terms power output and efficiency. Heppenstall [28] concluded that ammonia-water mixture cycle is unaffected by the fuel price and can offer higher efficiencies. Moreover, exergy losses can also be reduced if ammonia water mixture is used instead of steam/water [29]. An ammonia concentration of 0.7 is recommended by various authors in the open literature [30-33]. Mohammadi et al. [34] performed exergy and advanced exergy analysis of ammonia-water power and cooling cycle. The authors concluded that conventional exergy method depicts that maximum exergy is destroyed in boiler but when the plant was analyzed by using advanced exergy analysis it depicts turbine as the thermodynamic element in which maximum exergy destruction takes place.

Kim et al. [35] while analyzing the heat recovery vapor generator (HRVG) concluded that keeping other parameters of HRVG constant and varying ammonia mass fraction and pressure, shows a non-linear temperature distribution of the ammonia-water mixture. Moreover, as the entropy generation increases, second law efficiency of HRVG decreases with increasing ammonia concentration or decreasing pressure of the mixture.

Research Gap and Problem Formulation

The existing literature indicates that both power cycles show potential advantages compared to the Rankine cycle.

However, there has been limited exploration of their combined use for power generation purposes. Consequently, this study aims to fill this gap by examining the coupled cycle, specifically the combination of ammonia-water with T-CO_2, with a focus on power generation. The analysis will be based on evaluating the first and second law efficiency to provide a comprehensive understanding of the system's performance.

CYCLE ARRANGEMENTS

Figure 1 illustrates the schematic layout of the proposed cycle. The process begins with the liquid ammonia-water mixture, which undergoes heat exchange within the heat source (from state 10 to state 1). The heat source assumed here is the waste heat from the gas turbine. The mixture enters the ammonia-water turbine (which is an axial flow turbine) in vapor phase, where work is extracted (from state 1 to state 2). Subsequently, the ammonia-water mixture proceeds to the heat recovery vapor generator (HRVG), where it transfers heat to the liquid carbon dioxide (from state 2 to state 3).

The ammonia-water mixture then enters the absorber, where it is combined with the weak mixture (state 12) coming from the separator.

The mixing process between the weak mixture and the mixture from state 3 is exothermic, necessitating cooling to remove the heat generated. After the absorber, the resulting solution, known as the working solution, is pumped up, by pump P2, to the separator (from state 4 to state 5). In the separator, heat is provided to facilitate the movement of the rich solution to the feed heater (from state 6 to state 7), while the weak mixture flows back to the absorber through an expansion valve (from state 11 to state 12). Once passing through the feed heater, the rich mixture is cooled in the condenser (from state 7 to state 8). After being pumped by pump P1, (from state 8 to state 9) and carrying heat from the feed heater (state 9 to state 10), this mixture proceeds to the HRVG.

In the bottoming cycle, the working fluid changes to carbon dioxide, which is converted to supercritical carbon dioxide in the HRVG after extracting heat from the ammonia-water mixture (from state 17 to state 13). Work is then extracted from the transcritical carbon dioxide (from state 13 to state 14, through an axial flow turbine), and it is directed to the heat exchanger (HE) to obtain cooling from

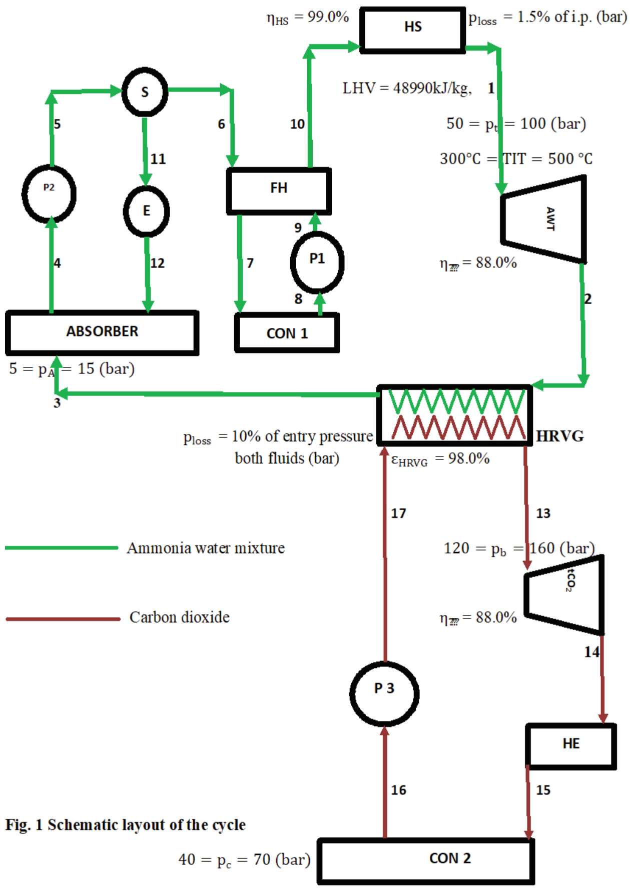

Figure 1. Schematic layout of the proposed cycle.

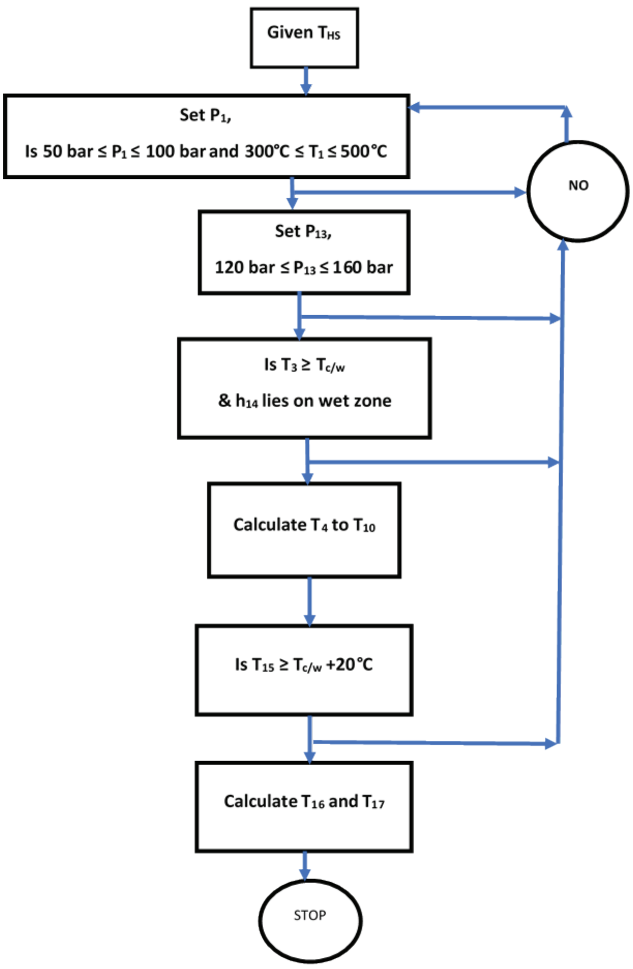

Figure 2. Flow chart for calculating temperature and hence enthalpy at various salient points.

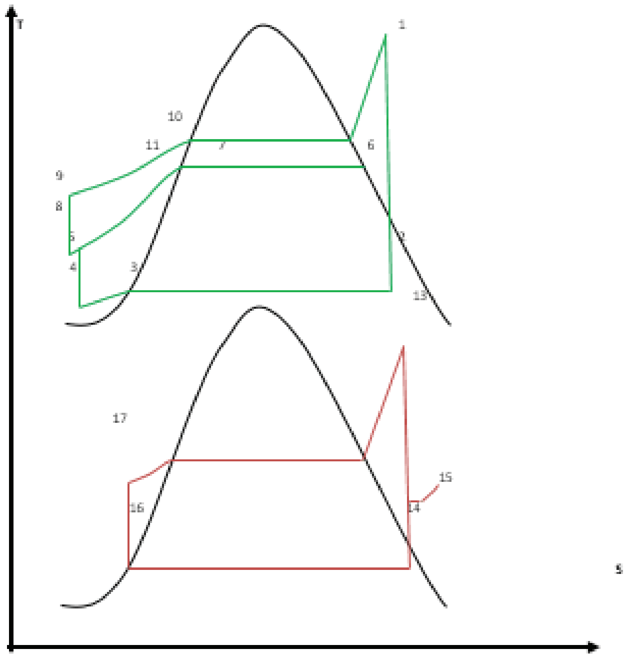

Figure 3. T-s plot for Figure 1.

the carbon dioxide (from state 14 to state 15). The carbon dioxide becomes a liquid as it rejects heat in the condenser (from state 15 to state 16) and is then pumped through pump P 3, (from state 16 to state 17) before returning to the HRVG.

Thermodynamic Modelling

Following assumptions were considered in the analysis of combined cycle

- Saturated liquid ammonia-water mixture enters the absorber.
- Corrosive effect due to ammonia-water mixture is not considered.
- Ammonia mass fraction at inlet to ammonia water turbine is 0.7
- The components of combined cycle under steady-state and steady-flow.
- Pinch point [Minimum temperature difference required to transfer heat] is taken to be 20.0°C [36]

The base parameters considered for analysis is shown on schematic layout of the cycle, i.e., Figure 2. Thermodynamic modelling associated with the given layout is presented in tabular form in Table 1. The performance parameters for evaluation of the cycle is provided from eq. (1) to eq. (5).

$$W_{\frac{sCO2}{amwt},net} = W_{sCO2/amwt} - \frac{W_{pump(s)}}{\eta_{pump}} \tag{1}$$

$$W_{combined\ cycle} = [W_{sCO_2t,net} + W_{amwt,net}]. \tag{2}$$

$$\eta_{I,combined\ cycle} = \frac{W_{combined\ cycle} + \frac{Q_{cool}}{\eta_{II,ref}}}{m_f CV} \tag{3}$$

Where $\dot{Q}_{cool} = \dot{m}[h_{tCO_2,in} - h_{tCO_2,out} - T_o(s_{a,in} - s_{a,out})]$ [43]

$$\eta_{II,combined\ cycle} = \frac{W_{combined\ cycle} + Q_{cool}}{\dot{m_f}.G_r} \tag{4}$$

$$\eta_{II,RHE} = \frac{\text{Exergy of outgoing fluids}}{\text{Exergy of incoming fluids}} \tag{5}$$

RESULTS AND DISCUSSION

Based on the thermodynamic modeling and base parameters selected following results are obtained.

Variation of work output, first law efficiency and second law efficiency for varying topping cycle pressure is depicted in Figure 2. The attributes of the graph depict that as the topping cycle pressure increases work output of the combined cycle decreases because with increase in topping cycle pressure, the exhaust temperature from the ammonia water cycle increases. This increase in exhaust temperature increases the enthalpy at exit to topping cycle, hence a reduced work output from ammonia-water cycle.

In bottoming cycle, increase in exhaust temperature from ammonia-water cycle, increases the turbine inlet temperature as well as mass flow rate of carbon-dioxide. But, the decrease in topping cycle work output is more as compared to the increase in bottoming cycle work output. Thus, observing a reduced work output in combined cycle.

The first law efficiency of the combined cycle is observed to be almost constant (change of 0.002% when going from 50bar to 100 bar), because the decrease in work output is less, 3.9% as compared to increase in pressure. Thus, small decrease in work output of the combined cycle does not produces any significant change in first law efficiency.

The second law efficiency is observed to 81% and almost constant. The high second law efficiency is obtained because of temperature glide nature of ammonia-water mixture and tCO_2.Moreover ammonia-water mixture shows a temperature glide in absorber, heat source, and condenser, which decreases the total irreversibility, associated with the topping cycle and hence increase in second law efficiency.

The attributes of the graph also depict that a marginal decrease in cost of electricity produced is observed as the topping cycle pressure increases from 50bar to 100bar.

Figure 3 depicts the irreversibility variation produced in different components of combined power cycle for varying topping cycle pressure. The attributes of Figure 3 shows that as the topping cycle pressure is increased the randomness of the working fluid particles entering the topping cycle turbine decreases. Whereas the entropy generation rate of bottoming cycle turbine is constant. This results in

Table 1. Thermodynamic of different components used in layout

Component	First law equations	Irreversibility associated with component	Cost function [37-42]
Heat Source	$\dot{m}_f.\,LHV.\,\eta_{HS} = \dot{m}_{amw}[h_{amw,e} -.\,h_{amw,i}]$	$\dot{I}_{HS} = T_o.\,\dot{m}_{amw}[s_{amw,e} - s_{amw,i}]$	$C_{HS} = \frac{46.08.\,\dot{m}_f}{0.995 - \left(\frac{P_{e,HS}}{P_{i,HS}}\right)}[1 + \exp(0.018.\,T_{e,HS} - 26.4)]$
Turbine(s)	$W_{\frac{tCO2}{amw},t} = \left[\dot{m}_{\frac{tCO2}{amw},t}.\,\eta_{is}\left(h_{\frac{tCO2}{amw},t,i} - h_{\frac{tCO2}{amw},t,e}\right)\right]$	$\dot{I}_{\frac{tCO2}{amw},t} = T_o.\,\dot{m}_{\frac{tCO2}{amw},t}.[\left(s_{\frac{tCO2}{amw},t,i} - s_{\frac{tCO2}{amw},t,e}\right)]$	$C_{\frac{tCO2}{amw},t} = 6000.\,(W_{tCO2} + W_{amwt})^{0.7}$
Pump(s)	$W_{pump,actual} = \frac{w_{is,pump}}{\eta_{is,pump}}$	$\dot{I}_{pump} = T_o\left[\dot{m}_{\frac{tCO2}{amw}}(s_o - s_i)\right]$	$C_{pump} = 705.48.\,({W_{pump}}^{0.71}).\,(1 + \frac{0.2}{1-\eta_{pump}})$
Condenser	$\dot{m}_{cw}(\dot{h}_{cw,e} - \dot{h}_{cw,i}) = \dot{m}_{\frac{tCO2}{amw}}.\left(h_{\frac{tCO2}{amw}} - h_{\frac{tCO2}{amw}}\right)$	$\dot{I}_{condenser} = T_o\left[\sum_j \dot{m}_j.\,(s_{j,i} - s_{j,o}) - m_{cw}c_{p,cw}\ln\frac{T_{cw/i}}{T_{cw/o}}\right]$	$C_{tCO2/amw} = 1773.\,\dot{m}_w$
Heat exchanger	$m_a(h_i - h_o) = \dot{m}_{tCO2}(h_{tCO2,o} - h_{sCO2,i})$	$\dot{I}_{HE} = T_o.[\dot{m}_{tCO2}.\,(s_{tCO2,o} - s_{tCO2,i}) - \dot{m}_{air}.\,(s_o - s_i)]$	$C_{HE} = 4745.\left(\frac{\dot{Q}_{HE}}{\log\Delta T_{HE}}\right)^{0.8} + 23640.\,\dot{m}_{amw}$
Feed heater	$(h_{r/sol.,i} - h_{r/sol.,o}) = (h_{wo/sol.,o} - h_{wo/sol.,i})$	$\dot{I}_{FH} = (s_{r/sol.,i} - s_{r/sol.,o}) - (s_{wo/sol.,o} - s_{wo/sol.,i})$	$C_{FH} = 4745.\left(\frac{\dot{Q}_{FH}}{\log\Delta T_{FH}}\right)^{0.8} + 23640.\,\dot{m}_{amw}$
Absorber	$m_{r/sol.}(h_{r/sol.,i} - h_{mix}) + m_{we/sol.}(h_{we/sol.,i} - h_{mix}) = 0$	$I_{Absorber} = T_o\left[\dot{m}_{wo/sol.}(s_{mix,i} - s_{mix,o}) - m_{cw}c_{p,cw}\ln\frac{T_{cw/i}}{T_{cw/o}}\right]$	$C_{Absorber} = 130.\left(\frac{A_{abs.}}{0.093}\right)^{0.78}$
HRVG	$\dot{m}_{tCO2}(c_{p,tCO2,e}t_{tCO2,e} - c_{p,tCO2,i}t_{tCO2,i}) = \dot{m}_{amw}(h_e - h_i)$	$\dot{I}_{HRVG} = T_o[\dot{m}_{tCO2}(s_{tCO2.,i} - s_{tCO2,o}) - \dot{m}_{amw.}(s_{amw,o} - s_{amw.,i})]$	$C_{HRVG} = 4745.\left(\frac{\dot{Q}_{HRVG}}{\log\Delta T_{HRVG}}\right)^{0.8} + 11820.\,(\dot{m}_{sCO_2} + \dot{m}_{amw}) + 658.\,\dot{m}_{fg}$
Cost of electricity generation	$\frac{\beta}{Po}.\frac{C}{H} + \frac{f}{\eta} + \left[\frac{OM_f}{Po.\,H} + \mu.\,OM_v\right]$ Where $\beta = \left[\frac{(1+d_e)^n - 1}{(1+d_e)^n.d_e}\right]\left[\frac{(1+d)^n.d}{(1+d)^n - 1}\right]$ and $f = \beta.\,(OM_f + OM_v)$, OM_v = Cost of fuel+ Cost of Ammonia water mixture		
Other parameters	Discount rate (d) = 10% Plant lifetime (n) = 10 Years Plant availability (H) = 8000 h/year (Depreciation rate) de = 4% Maintenance cost and escalation factor (μ) = 2.5		

J Ther Eng, Vol. 10, No. 3, pp. 599−612, May, 2024

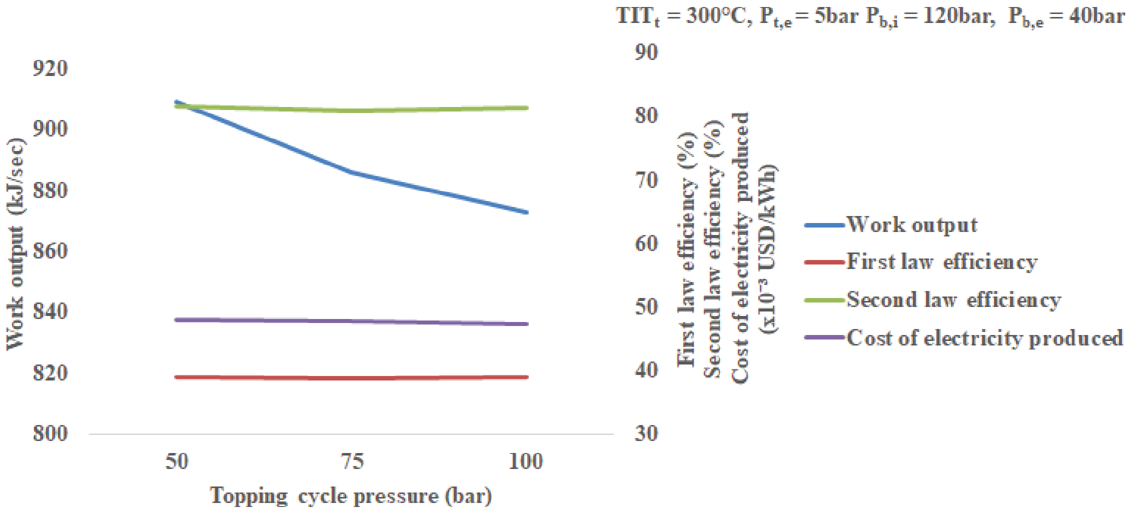

Figure 4. Variation of work output, first law efficiency, second law efficiency and cost of electricity produced with varying topping cycle pressure.

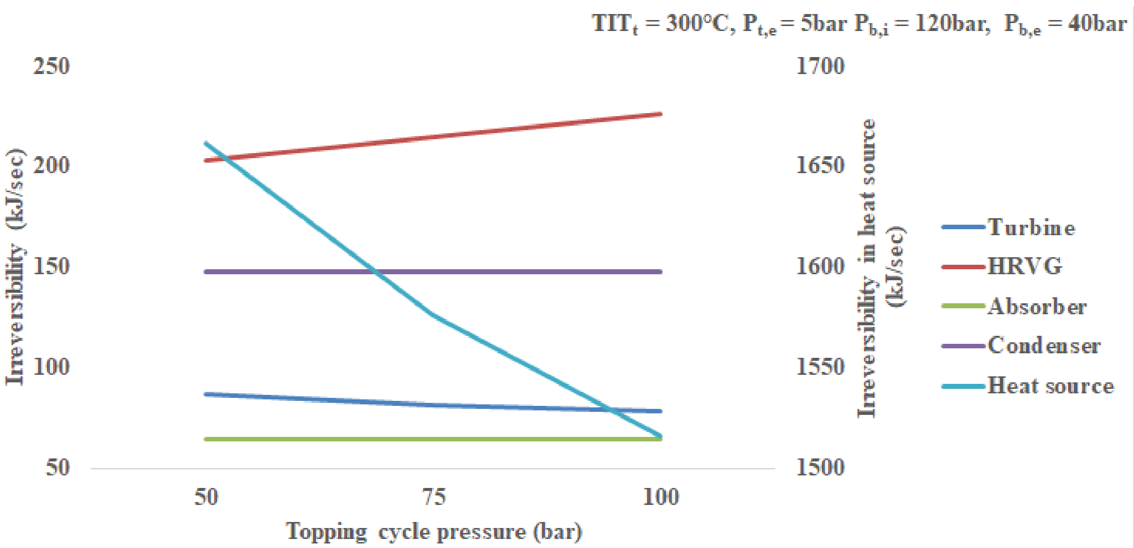

Figure 5. Variation in irreversibility produced in different components of combined power cycle with varying topping cycle pressure.

the decrease in irreversibility of both the turbines, taken together and the heat source.

In HRVG section as the topping cycle pressure increases the exhaust temperature from the ammonia-water cycle decreases. This increase in temperature increases the irreversibility in HRVG section.

As the pressure increases the exhaust temperature from the turbine decreases thus resulting in lower exit temperature from HRVG. When this low temperature mixture enters the absorber there is decrease in mass flow rate of cooling water required, thereby decreasing the entropy generation and hence irreversibility in absorber.

Whereas exergy destroyed in COND 1 i.e., condenser of topping cycle is constant because of no change in temperature at which heat is added in separator. In bottoming cycle, since the variation observed in exit temperatures from the turbine and heat exchanger are negligible hence the cooling water flow rate required does not vary thereby observing no significant change in irreversibility of COND 2.

For constant turbine inlet temperature, as the pressure increases the change in entropy decreases which decreases the irreversibility associated with the heat source.

The effect of bottoming cycle pressure on work output, first law efficiency, second law efficiency and irreversibility (in different thermodynamic element) are depicted in

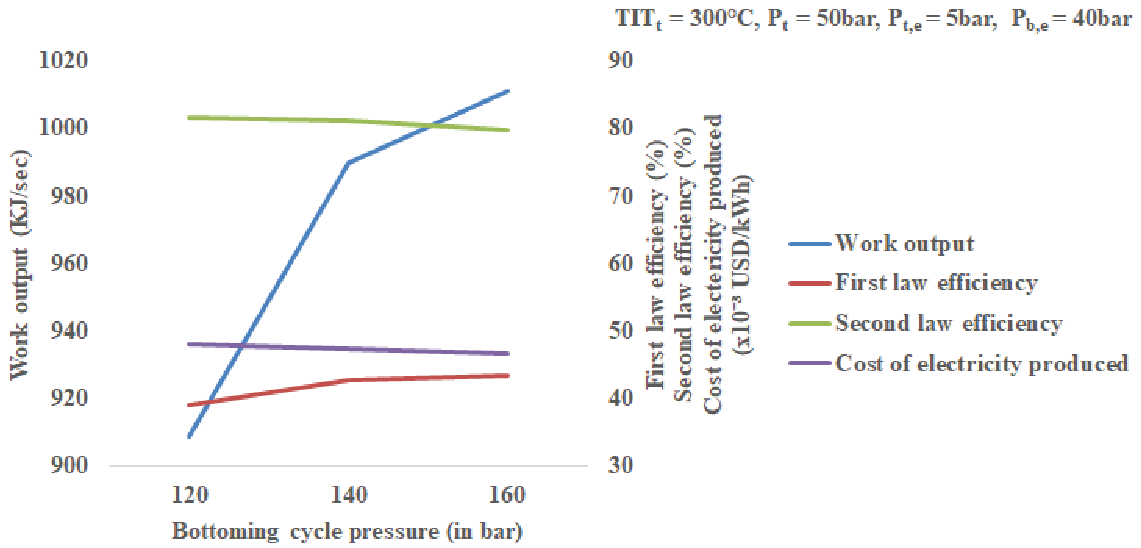

Figure 6. Variation of work output, first law efficiency, second law efficiency and cost of electricity produced with varying bottoming cycle pressure.

Figure 4 and Figure 5 respectively. The attributes of the graph predict that increase in bottoming cycle pressure increases the work output of the combined cycle (Figure 4). Since, the increase in pressure of the bottoming cycle decreases the enthalpy at inlet to the turbine but an increase in the mass flow rate is observed. This increase in mass flow rate results in increased work output of the bottoming cycle and hence the combined cycle.

An increase in work output results in increase in cycle efficiency of the combined cycle. The cost of electricity produced decreases with increase in bottoming cycle pressure. The second law efficiency of the combined cycle with increase in bottoming cycle pressure increases (Figure 4) and reaches a maximum value of 79.2% at a pressure of 120bar. The increase in second law efficiency may be due to (Figure 5).

- Decrease in irreversibility of the turbine with increase in bottoming cycle pressure.
- An increase in irreversibility of HRVG is observed as bottoming cycle pressure increases. Since, entropy generated due to ammonia-water mixture is constant and with increase in pressure the randomness of CO_2 molecules decreases, this implies that increase in

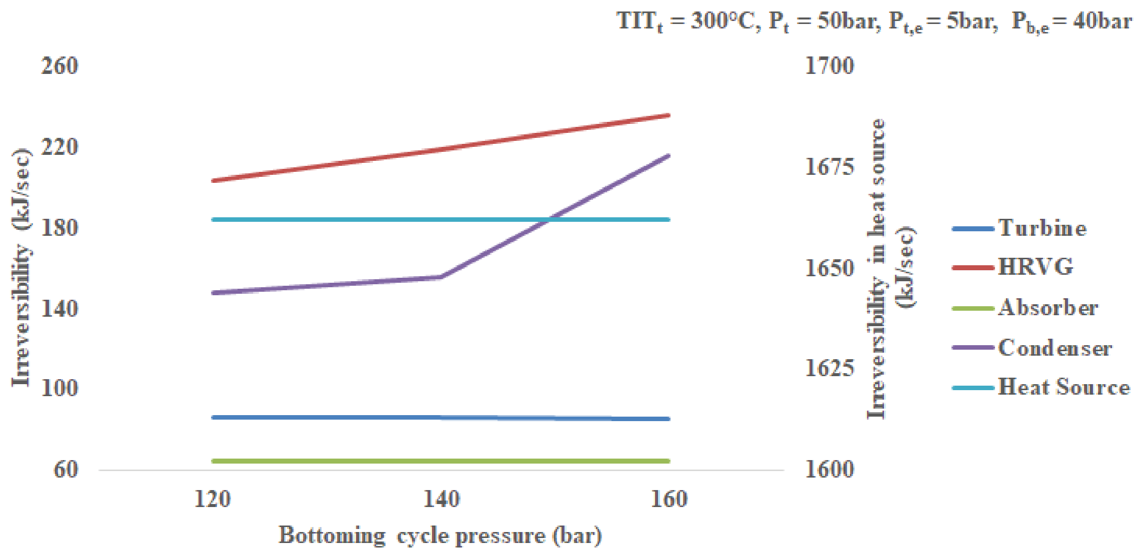

Figure 7. Variation in irreversibility produced in different components of combined power cycle with varying bottoming cycle pressure.

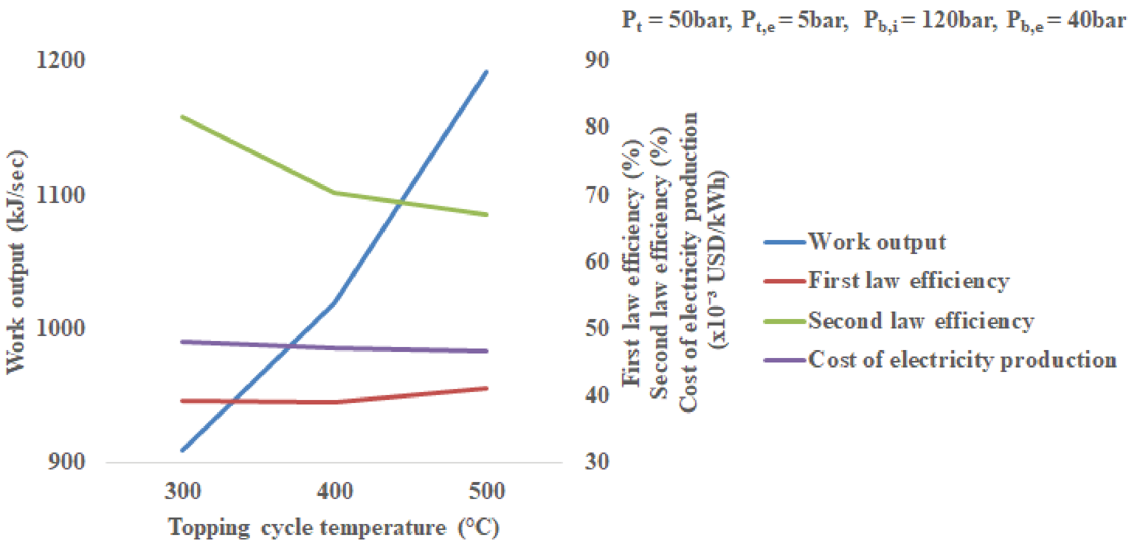

Figure 8. Variation of work output, first law efficiency, second law efficiency and cost of electricity produced with varying topping cycle temperature.

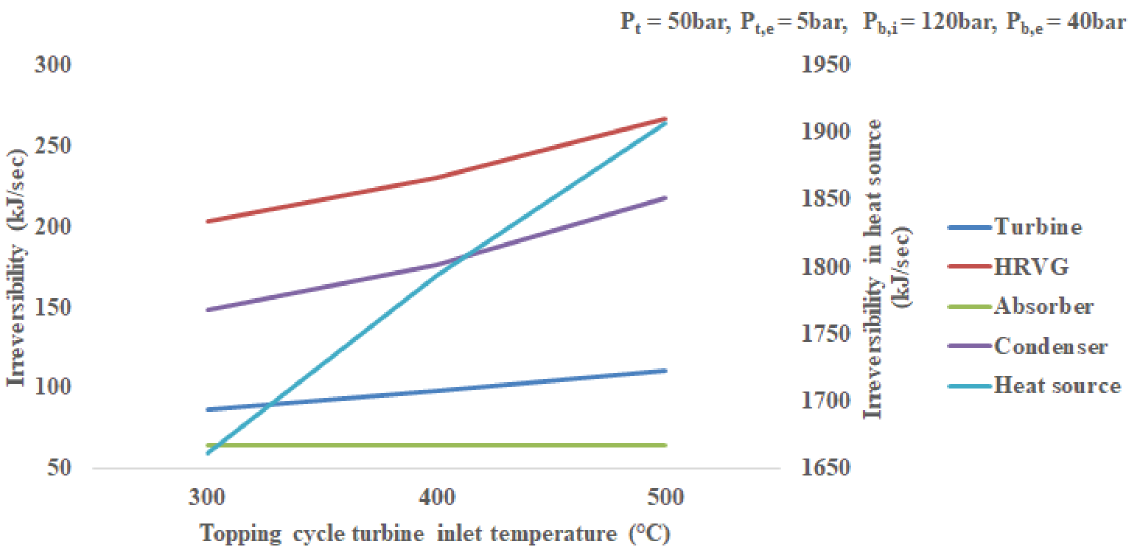

Figure 9. Variation in irreversibility produced in different components of combined power cycle with varying topping cycle temperature.

irreversibility is attributed due to increased mass flow rate of bottoming cycle working fluid.

- Absorber and heat source are not affected by the change in bottoming cycle pressure.
- Considering the irreversibility in condenser, Figure 5 depicts that as the bottoming cycle turbine inlet pressure increases irreversibility in condenser increases. The increase in irreversibility of condenser may be because of
- Increased mass flow rate through the bottoming cycle and
- The increase in exhaust temperature from the CO_2 turbine.

The increase in turbine inlet temperature of ammonia-water cycle increases the work output of the combined cycle and reaches to a maximum value of 1192kJ/sec., correspondingly the cycle efficiency also increases due to increased work output. Deviation is observed in second law efficiency, where it decreases, as turbine inlet temperature increases, (Figure 6).

As depicted in Figure 6 that a deviation is observed in second law efficiency this deviation may be due to (Figure 7)

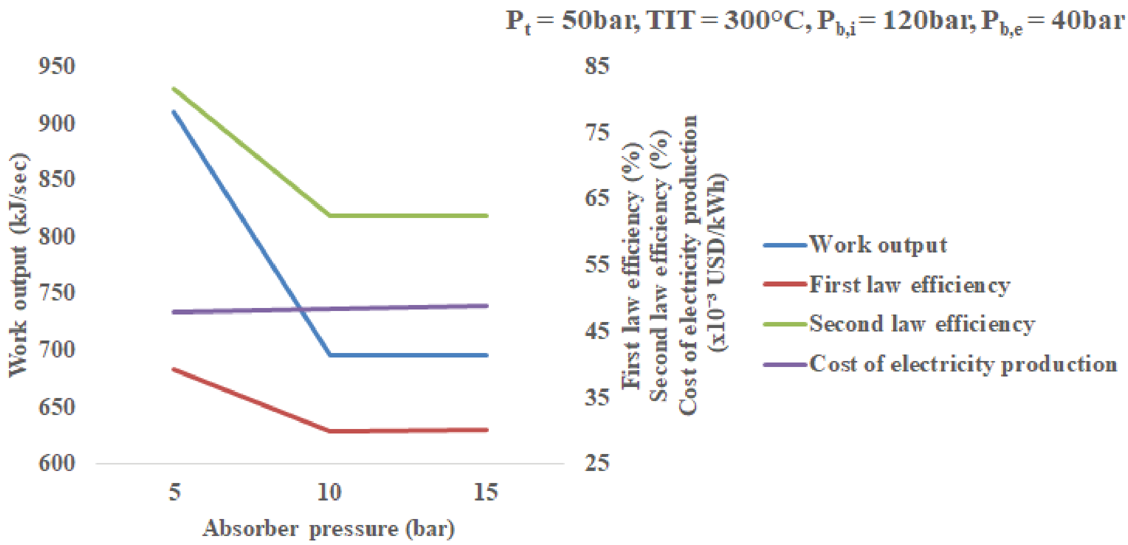

Figure 10. Variation of work output, first law efficiency, second law efficiency and cost of electricity produced with varying absorber pressure.

Increase in irreversibility of turbine, which increases with increase in turbine inlet temperature for constant pressure in ammonia-water cycle.

In bottoming cycle, due to high inlet temperature in topping cycle consequently increases the inlet temperature to CO_2 cycle, resulting an increase in irreversibility of bottoming cycle turbine also. Thus, an overall increase in irreversibility of turbine due to increase in exhaust temperature from heat source.

Due to increase in temperature from heat source, the enthalpy at exit to ammonia-water turbine increases. Since, it is assumed that saturated liquid will enter the absorber, thus resulting in an increase in exergy destruction in HRVG section. Moreover, mass flow rate of CO_2 also increases with increase in temperature there by adding irreversibility to HRVG.

As the turbine inlet temperature increases, condenser handles the increased mass flow rate of both – the working fluid and the cooling water. Also, the exhaust temperature from CO_2 turbine increases. Thus, increase in temperature and mass flow rate (of both fluids) increases the irreversibility in condenser.

The main source of energy destruction is the heat source. Figure 7 depicts that as the turbine inlet temperature increases, the unavailable energy increases and reaches its maximum value for a temperature of 500°C.

The increase in absorber pressure from 5bar to 10bar decreases the work output thereafter marginal increase is observed in, as pressure increases from 10 bar to 15 bar, (Figure 8). This may be attributed because of decrease in work output in topping cycle is more as compared to the gain obtained due to increase mass flow rate in bottoming cycle. But as the pressure increases beyond 10 bar the gain in work output of the bottoming cycle increases, as compared to the drop in topping cycle there by observing a marginal gain in work output.

Cycle efficiency and second law efficiency follows the same pattern as that of work output.

Figure 11 depicts the irreversibility associated with change in absorber pressure. The attributes of the graph depict that as the absorber pressure increases irreversibility in HRVG increases because of increase in inlet temperature of HRVG and hence increased mass flow rate of CO_2.

Due to the mixing of weak ammonia-concentration coming from separator and rich concentration mixture coming from HRVG, heat is being rejected from the absorber. This phenomenon of heat rejection increases with increase in absorber pressure, thus an increase in irreversibility in absorber due to increase in absorber pressure. Irreversibility in condenser also increases as the absorber pressure increases.

Figure 12 depicts that the increase in condenser pressure from 40 bar to 70 bar decreases the work output of the bottoming cycle and hence the combined cycle. Due to decrease in work output, cycle efficiency and second law efficiency also follows the same trend. The cost of electricity produced increases as the condenser pressure increases.

Variation in irreversibility produced in different components of combined power cycle with varying bottoming cycle condenser pressure is depicted in Figure 13. The graphical attributes depict that heat source, absorber and HRVG are unaffected by the change in bottoming cycle condenser pressure. Due to increase in irreversibility of bottoming cycle turbine, the total irreversibility of both the turbine increases.

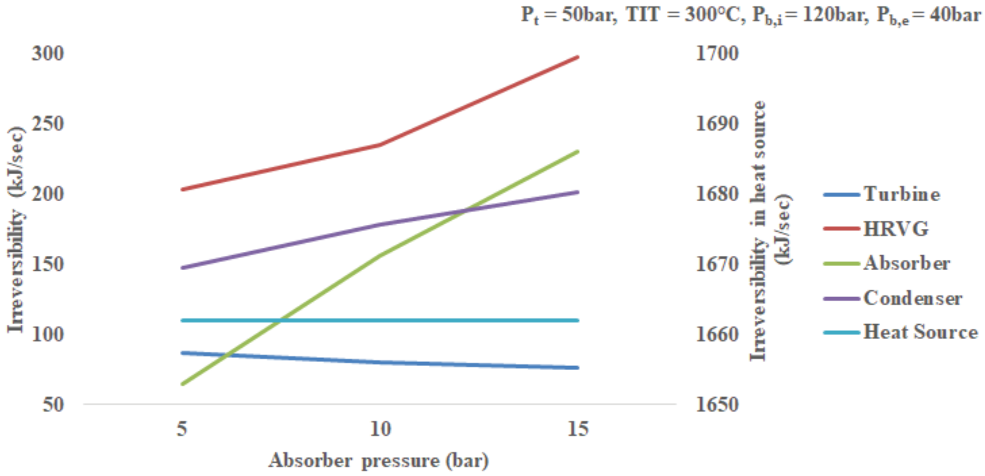

Figure 11. Variation in irreversibility produced in different components of combined power cycle with varying absorber pressure.

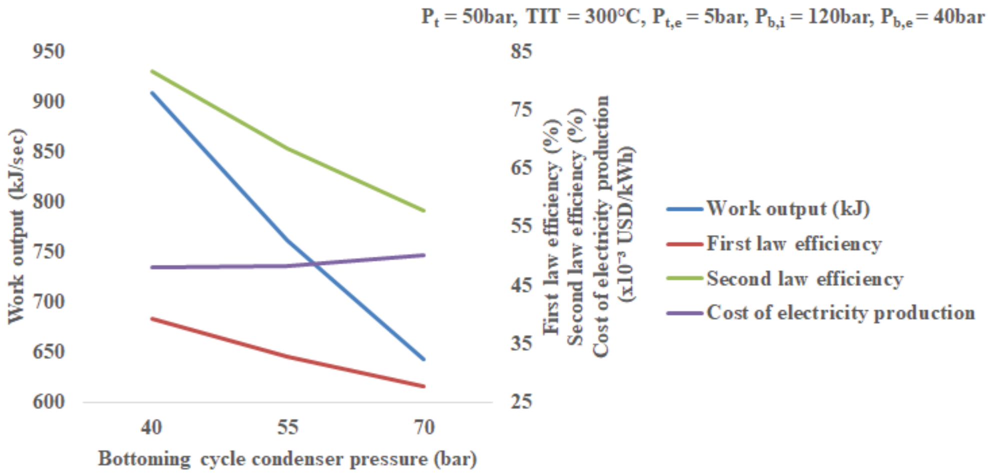

Figure 12. Variation of work output, first law efficiency, second law efficiency and cost of electricity produced with varying bottoming cycle condenser pressure.

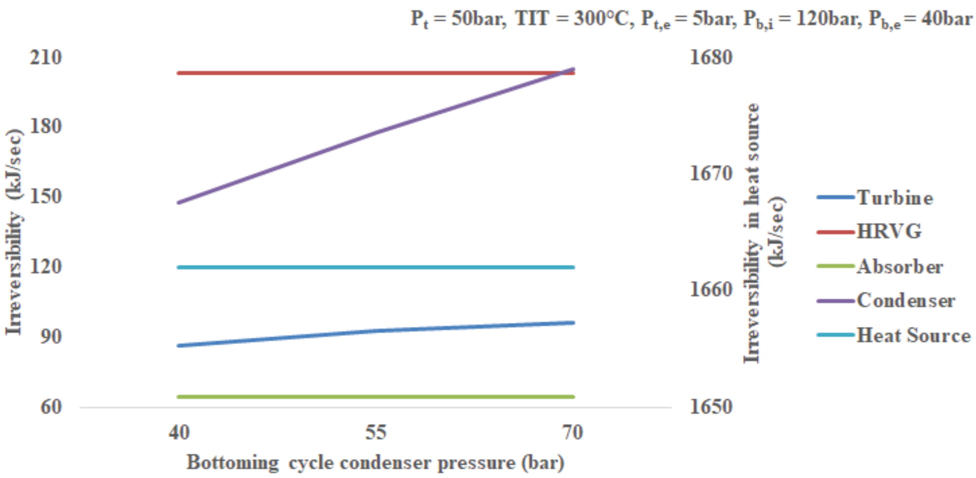

Figure 13. Variation in irreversibility produced in different components of combined power cycle with varying bottoming cycle condenser pressure.

Irreversibility Increases in Condenser due to Increased Temperature of Working Fluid

Figure 14 shows depicts the exergy destroyed in terms of exergy input and cost of exergy destruction. The diagram depicts that heat source share the maximum cost of exergy destruction.

Validation

The present work is compared with the works of Su et al. [44] in Figure 13. Su et al. depicts a first and second law efficiency as 30.74% and 61.55% at 505°C as compared to the 41.2% and 68.26% (of the present work) at 500°C. This substantial difference may be because of the authors using ammonia water absorbtion cycle for producing cooling

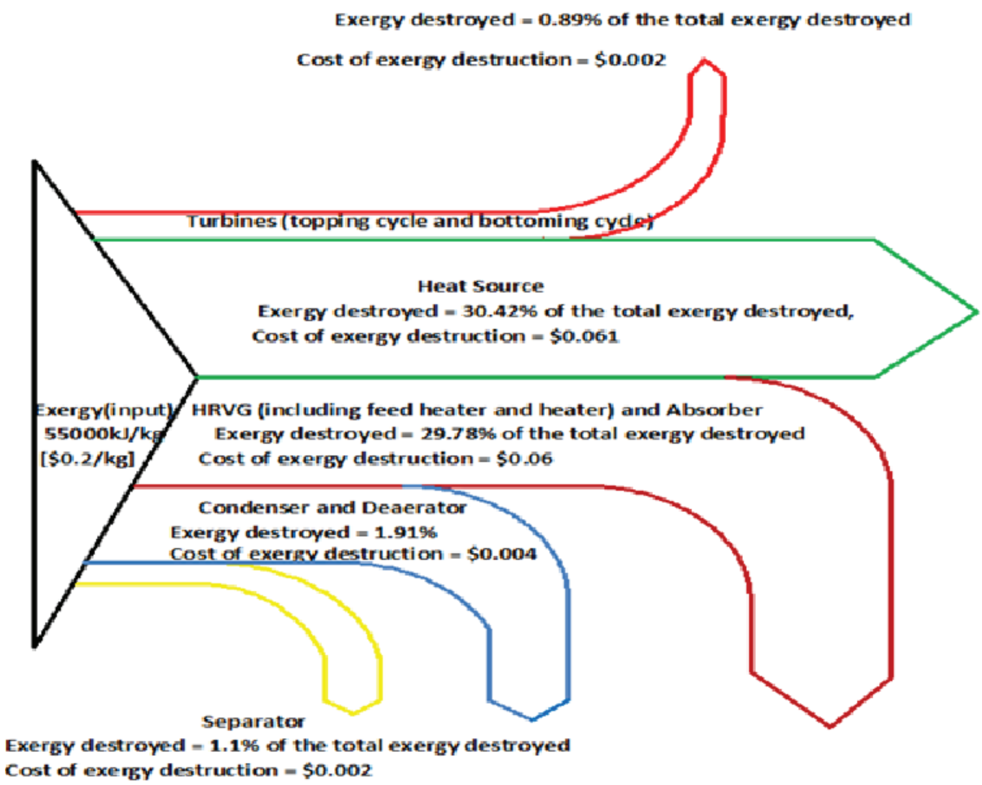

Figure 14. E-Sankey diagram for the exergy destruction along with the cost associated in different components of proposed layout.

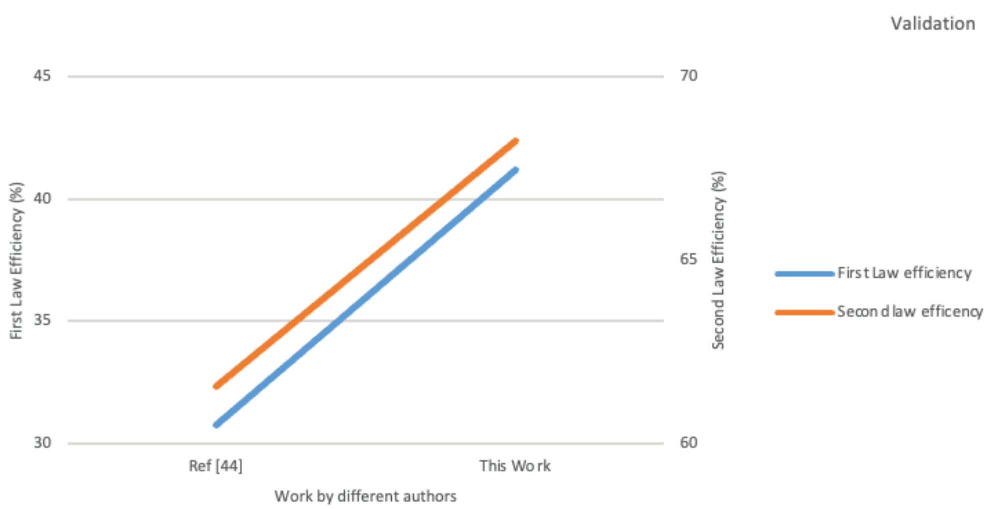

Figure 15. Validation of present work with that of ref. [44].

effect due to which a loss in work, hence the loss in first and second law efficiency take place. Whereas cooling effect is considered in present work.

CONCLUSION

Thermodynamic analysis of ammonia-water mixture cycle coupled with tCO_2 cycle is performed from energy, exergy and economical point of view. This binary vapor power cycle can maximize the use of fuel energy i.e., increase in first and second law efficiency of the power cycle. Following conclusions are drawn by varying topping cycle turbine pressure and temperature, absorber pressure, bottoming cycle turbine inlet pressure, condenser pressure:

- As the topping cycle pressure increases, by keeping other parameters constant (TIT_t = 300°C, $P_{t,e}$ = 5bar $P_{b,i}$ = 120bar, $P_{b,e}$ = 40bar), then maximum work output of 909kJ/sec. and first law efficiency is obtained at 50bar while second law efficiency of 81.64% is obtained at 100 bar.
- If bottoming cycle pressure is changed from 120 bar to 160 bar, then work output and first law efficiency of 1011kJ/sec. and 43.57% is obtained but second law efficiency reduced to 79% for the same conditions.
- The increase in turbine inlet temperature from 300°C to 500°C increases the work output from 909kJ/sec. to 1192kJ/sec. but decreases the second law efficiency up to 67.15%
- Increase in absorber pressure and condenser pressure not only lowers the work output of the combined cycle but reduces the cycle efficiency and second law efficiency to below 30% and 60% respectively.
- Heat source forms the major source of exergy destruction with its maximum value upto 1970kJ/sec for P_t = 50bar, $P_{t,e}$ = 5bar, $P_{b,i}$ = 120bar, $P_{b,e}$ = 40bar and T_t =500°C.
- Cost of electricity goes up to 0.0501USD/kWh for P_t = 50bar, TIT = 300°C, $P_{t,e}$ = 5bar, $P_{b,i}$ = 120bar, $P_{b,e}$ = 40bar

Scope of Future Works

The present work analyses a binary vapor power cycle using ammonia-water mixture and T-CO_2. This cycle can further be investigated as in combination with a gas turbine. Furthermore, exergy analysis can also be performed using non-conventional energy source such as solar energy.

NOMENCLATURE USED

Specification Symbol

Symbol	Specification	Unit (Dimensions)
C	Cost function	-
CV	Calorific value of fuel	kJ/kg
c_p	Specific heat at constant pressure	kJ/kg.K
d_e	Depreciation factor	-
f	Variable used in economic analysis	-
h	Enthalpy	kJ/kg
HE	Heat exchanger	-
HRVG	Heat recovery vapor generator	-
$\dot{I}$	Irreversibility	kJ/sec
LHV	Lower heating value	kJ/kg
$\dot{m}$	Mass flow rate	kg/second
OM	Operation and maintenance	-
p/P	Pressure	bar
$\dot{Q}$	Refrigerating effect	kJ/sec
s	Entropy	kJ/kg.K
sCO_2	Super critical carbon dioxide	-
T/t	Tran-critical (when used with CO_2)/Temperature	°C
W	Work produced/consumed by turbine/pump	kJ/sec
T_o, P_o	Dead state temperature and pressure respectively	in °C and bar

Abbreviations Used in text/layout:

Symbol	Specification	Unit (Dimensions)
a	air	-
AWT	Ammonia water turbine	-
CON	Condenser	-
CV	Calorific value	-
E	Expansion valve	-
FH	Feed Heater	-
HE	Heat exchanger	-
HS	Heat source	-
HRVG	Heat Recovery Vapour Generator	-
OM_F	Fixed operation and maintenance cost for base load operation	-
OMV	Variable operation and maintenance cost for base load operation	-
P (1,2,3)	Pump	-
Q	Heat input	kJ/sec
S	Separator	-
TIT	Turbine inlet temperature	°C
TCO_2	Trans critical carbon dioxide	-
i.p	Input pressure	bar

Greek Symbols:

Symbol	Specification	Unit (Dimensions)
η	Efficiency	%
Δ	Difference	-
β	Variable used in economic analysis	-
ε	Effectiveness of heat exchanging element	-

Subscripts

Symbol	Specification
a	Air
A	Absorber
amw	Ammonia Water Mixture

b	Bottoming
c	Condenser
cw	Cooling Water
e/o	Exit/outlet
f	Fuel
FH	Feed heater
HE	Heat exchanger
HS	Heat source
i	Inlet
is	Isentropic
j	Summation over both the condenser i.e., CON 1 and CON 2
mix	Mixture
p	Polytrophic (if not used with 'c')
p	Pump
r	Rich
ref	Refrigerating effect
sol.	Solution
sCO_2	Super critical carbon dioxide
tCO_2	Trans critical carbon dioxide
t	turbine/topping
v	Variable cost
we	Weak
wo	working

AUTHORSHIP CONTRIBUTIONS

Authors equally contributed to this work.

DATA AVAILABILITY STATEMENT

The authors confirm that the data that supports the findings of this study are available within the article. Raw data that support the finding of this study are available from the corresponding author, upon reasonable request.

CONFLICT OF INTEREST

The author declared no potential conflicts of interest with respect to the research, authorship, and/or publication of this article.

ETHICS

There are no ethical issues with the publication of this manuscript.

REFERENCES

[1] Kalina AI. Combined-cycle system with novel bottoming cycle. J Eng Gas Turbines Power 1984;106:737−742. [CrossRef]
[2] Angelino G. Carbon dioxide condensation cycles for power production. J Eng Power 1968;90:287−295. [CrossRef]
[3] Feher EG. The supercritical thermodynamic power cycle. Energy Convers Manag. 1968;8:85−90. [CrossRef]
[4] Turchi CS, Ma Z, Neises TW, Wagner MJ. Thermodynamic study of advanced supercritical carbon dioxide power cycles for concentrating solar power systems. J Sol Energy Engineer 2013;135:041007. [CrossRef]
[5] Wang J, Huang Y, Zang J, Liu G. Recent research progress on supercritical carbon dioxide power cycle in China. In: Asme Conference Proceedings. Proceedings of the Turbo Expo: Power for Land, Sea, and Air (Vol. 56802, p. V009T36A016). American Society of Mechanical Engineers; 2015.
[6] Dostal V, Driscoll MJ, Hejzlar P, Todreas NE. A supercritical CO_2 gas turbine power cycle for next-generation nuclear reactors. In: International Conference on Nuclear Engineering; Vol 35960; 2002. pp. 567−574. [CrossRef]
[7] Ahn Y, Lee J, Kim SG, Lee JI, Cha JE, Lee SW. Design consideration of supercritical CO_2 power cycle integral experiment loop. Energy 2015;86:115−127. [CrossRef]
[8] Dostal V, Hejzlar P, Driscoll MJ. The supercritical carbon dioxide power cycle: comparison to other advanced power cycles. Nucl Technol 2006;154:283−301. [CrossRef]
[9] Zhang XR, Yamaguchi H, Uneno D. Thermodynamic analysis of the CO_2-based Rankine cycle powered by solar energy. Int J Energy Res 2007;31:1414−1424. [CrossRef]
[10] Zhang XR, Yamaguchi H, Uneno D. Experimental study on the performance of solar Rankine system using supercritical CO_2. Renew Energy 2007;32:2617−2628. [CrossRef]
[11] Bozorgian AR. Analysis and simulating recuperator impact on the thermodynamic performance of the combined water-ammonia cycle. Prog Chem Biochem Res 2020;3:169−179. [CrossRef]
[12] Chen Y, Lundqvist P, Johansson A, Platell P. A comparative study of the carbon dioxide transcritical power cycle compared with an organic Rankine cycle with R123 as working fluid in waste heat recovery. Appl Therm Eng 2006;26:2142−2147. [CrossRef]
[13] Persichilli M, Kacludis A, Zdankiewicz E, Held T. Supercritical CO_2 power cycle developments and commercialization: Why sCO_2 can displace steam. Power-Gen India and Cent Asia, 19-21 Apr. 2012, New Delhi, India; 2012. pp. 19−21.
[14] Jeong WS, Lee JI, Jeong YH, No HC. Potential improvements of supercritical CO_2 Brayton cycle by modifying critical point of CO_2. Korean Nuclear Society Autumn Meeting, 29-30 October 2009, Gyeongju, Korea.
[15] Wang J, Sun Z, Dai Y, Ma S. Parametric optimization design for supercritical CO_2 power cycle using genetic algorithm and artificial neural network. Appl Energy 2010;87:1317−1324. [CrossRef]
[16] Li L, Ge YT, Luo X, Tassou SA. Thermodynamic analysis and comparison between CO_2 transcritical power cycles and R245fa organic Rankine cycles for

low grade heat to power energy conversion. Appl Therm Eng 2016;106:1290−1299. [CrossRef]

[17] Crespi F, Gavagnin G, Sánchez D, Martínez GS. Supercritical carbon dioxide cycles for power generation: a review. Appl Energy 2017;195:152−183. [CrossRef]

[18] Liao G, Liu L, E J, Zhang F, Chen J, Deng Y, et al. Effects of technical progress on performance and application of supercritical carbon dioxide power cycle: A review. Energy Conver Manage 2019;199:111986. [CrossRef]

[19] Mohammadi K, Ellingwood K, Powell K. A novel triple power cycle featuring a gas turbine cycle with supercritical carbon dioxide and organic Rankine cycles: Thermoeconomic analysis and optimization. Energy Conver Manage 2020;220:113123. [CrossRef]

[20] Habibollahzade A, Petersen KJ, Aliahmadi M, Fakhari I, Brinkerhoff JR. Comparative thermoeconomic analysis of geothermal energy recovery via super/transcritical CO_2 and subcritical organic Rankine cycles. Energy Conver Manage 2022;251:115008. [CrossRef]

[21] Yilmaz F, Ozturk M, Selbas R. Modeling and design of the new combined double-flash and binary geothermal power plant for multigeneration purposes; thermodynamic analysis. Int J Hydrog Energy 2022;47:19381−19396. [CrossRef]

[22] Sánchez D, Vidan-Falomir F, Larrondo-Sancho R, Llopis R, Cabello R. Alternative CO_2-based blends for transcritical refrigeration systems. Int J Refrig 2023;152:387−399. [CrossRef]

[23] Xu F, Goswami DY. Thermodynamic properties of ammonia-water mixtures for power-cycle applications. Energy 1999;24:525−536. [CrossRef]

[24] Cao L, Wang J, Wang H, Zhao P, Dai Y. Thermodynamic analysis of a Kalina-based combined cooling and power cycle driven by low-grade heat source. Appl Therm Engineer 2017;111:8−19. [CrossRef]

[25] El-Sayed YM, Tribus M. Thermodynamic properties of water-ammonia mixtures-theoretical implementation for use in power cycles analysis. Analysis of Energy Systems-Design and Operation; 1985.

[26] Marston CH, Hyre M. Gas turbine bottoming cycles: triple-pressure steam versus Kalina. J Eng Gas Turbines Power 1995;117:10−15. [CrossRef]

[27] Chen X, Wang RZ, Wang LW, Du S. A modified ammonia-water power cycle using a distillation stage for more efficient power generation. Energy 2017;138:1−11. [CrossRef]

[28] Heppenstall T. Advanced gas turbine cycles for power generation: a critical review. Appl Therm Engineer 1998;18:837−846. [CrossRef]

[29] Nag PK, Gupta AVSSKS. Exergy analysis of the Kalina cycle. Appl Therm Engineer 1998;18:427−439. [CrossRef]

[30] Valdimarsson P. Factors influencing the economics of the Kalina power cycle and situations of superior performance. International Geothermal Conference, Reykjavik, Sept 2003. pp. 32−40.

[31] Wall G, Chuang CC, Ishida M. Exergy study of the Kalina cycle. Anal Design Energy Sys: Anal Indust Process 1989;10:73−77.

[32] Desideri U, Bidini G. Study of possible optimisation criteria for geothermal power plants. Energy Conver Manage 1997;38:1681−1691. [CrossRef]

[33] Leibowitz HM, Mlcak HA. Design of a 2MW Kalina cycle binary module for installation in Husavik, Iceland. Trans Geotherm Resour Counc 1999:75−80.

[34] Mohammadi Z, Musharavati F, Ahmadi P, Rahimi S, Khanmohammadi S. Advanced exergy investigation of a combined cooling and power system with low-temperature geothermal heat as a prime mover for district cooling applications. Sustain Energy Technol Assess 2022;51:101868. [CrossRef]

[35] Kim KH, Ko HJ, Kim K. Assessment of pinch point characteristics in heat exchangers and condensers of ammonia-water based power cycles. Appl Energy 2014;113:970−981. [CrossRef]

[36] Maheshwari M, Singh O. Thermo-economic analysis of combined cycle configurations with intercooling and reheating. Energy 2020;205:118049. [CrossRef]

[37] Prakash D, Singh O. Thermo-economic study of combined cycle power plant with carbon capture and methanation. J Cleaner Prod. 2019;231:529−542. [CrossRef]

[38] Singh R, Singh O. Comparative study of combined solid oxide fuel cell-gas turbine-Organic Rankine cycle for different working fluid in bottoming cycle. Energy Conver Manage 2018;171:659−670. [CrossRef]

[39] Owebor K, Oko COC, Diemuodeke EO, Ogorure OJ. Thermo-environmental and economic analysis of an integrated municipal waste-to-energy solid oxide fuel cell, gas-, steam-, organic fluid-and absorption refrigeration cycle thermal power plants. Appl Energy 2019;239:1385−1401. [CrossRef]

[40] Campbell JM. Gas Conditioning and Processing, Vol. 1. The Basic Principals. 8th ed. Norman, OK: Campbell Petroleum Series; 2001.

[41] Gülen SC. A more accurate way to calculate the cost of electricity. Power. Available at: https://www.powermag.com/a-more-accurate-way-to-calculate-the-cost-of-electricity/. Accessed Apr 25, 2024.

[42] CERC. Tariff (Regulation) Norms 2014, Order No. L-1/144/2013/CERC.

[43] Maheshwari M, Singh O. Effect of atmospheric condition and ammonia mass fraction on the combined cycle for power and cooling using ammonia water mixture in bottoming cycle. Energy 2018;148:585−604. [CrossRef]

[44] Su R, Yu Z, Wang D, Sun B, Sun JN. Performance analysis of an integrated supercritical CO_2 recompression/absorption refrigeration/Kalina cycle driven by medium-temperature waste heat. J Therm Sci 2022;31:2051−2067. [CrossRef]